SSC-220

The Superconducting Super Collider

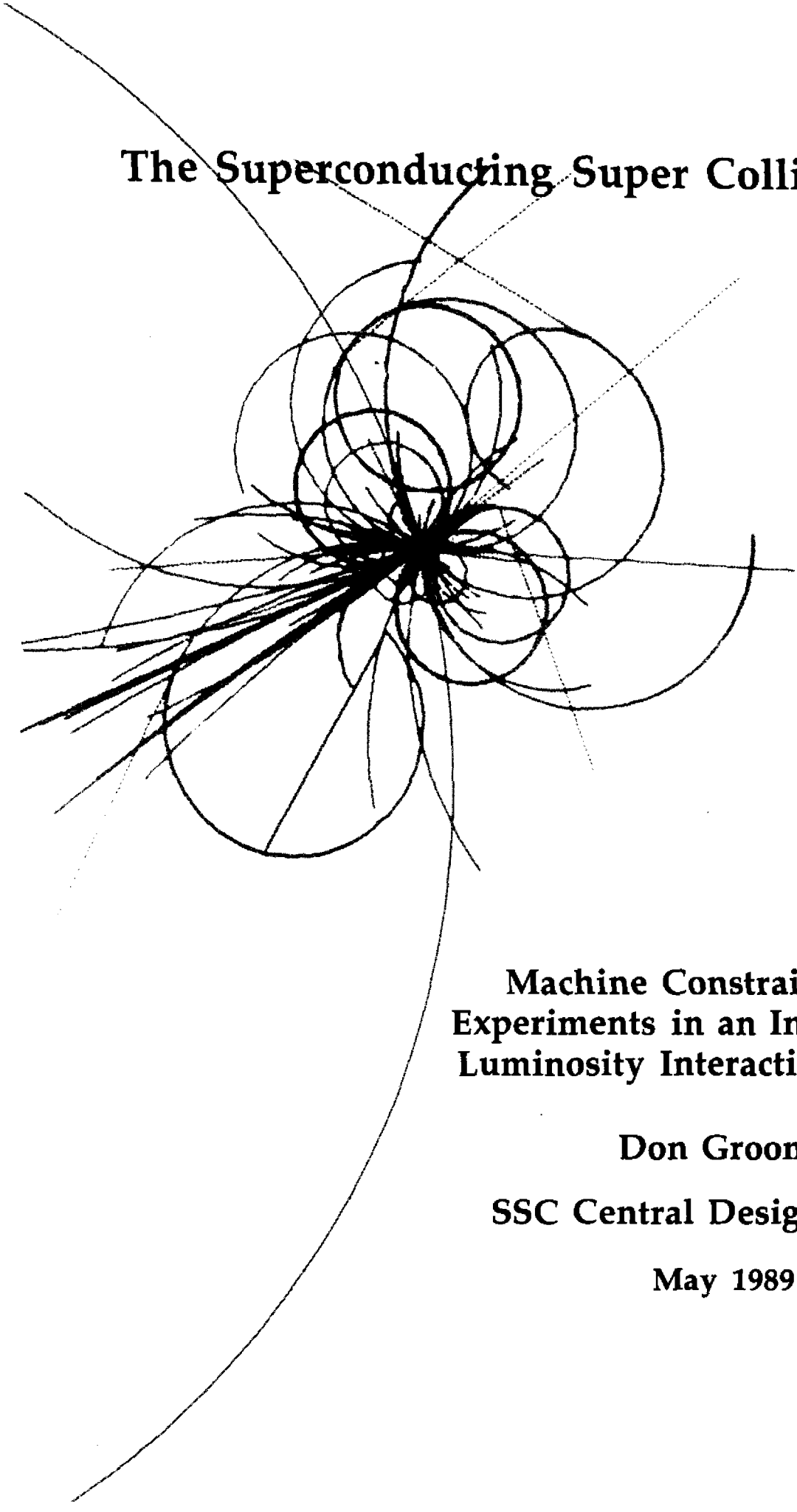

Machine Constraints for Experiments in an Intermediate Luminosity Interaction Region

Don Groom

SSC Central Design Group

May 1989

SSC-220

Machine Constraints for Experiments in an Intermediate Luminosity Interaction Region

Don Groom

SSC Central Design Group*
Lawrence Berkeley Laboratory
Berkeley, CA 94720

May 1989

* Operated by the Universities Research Association, Inc. for the Department of Energy.

SSC–220
23 May 1989

Machine Constraints for Experiments in an Intermediate Luminosity Interaction Region

Don Groom
SSC Central Design Group, LBL 90-4040, Berkeley CA 94720

We summarize existing information about the luminosity as a function of clear space between the interaction point and the front of the final-focus triplet, and about the minimum beam pipe dimensions (stay-clear dimensions) in the region.

1. Introduction

In the 1984 Snowmass report, Diebold and Johnson addressed the question of luminosity as a function of free space in an SSC interaction region [1]. They present a graph of $\beta^\star$ as a function of $L^\star$, the distance from the interaction point (IP) to the entrance of the first quadrupole. $\beta^\star$ rises smoothly from 1 m at $L^\star = 20$ m to 5 m at $L^\star = 100$ m. In contrast, the CDR [2] describes a high-luminosity interaction region (IR) with $\beta^\star = 0.5$ m and $L^\star = 20$ m, and an intermediate luminosity IR with $\beta^\star = 10$ m and $L^\star = 120$ m. No particular attempts were made to "tune" the intermediate IR for higher luminosity, but we are left with no information about the maximum attainable luminosity (or, better, the minimum attainable $\beta^\star$) as a function of $L^\star$. This problem has been addressed by Johnson in a somewhat different context, and one purpose of this report is to describe and qualify his results for purposes of planning experiments for an intermediate $\beta^\star$ IR.

At present, a forward B detector is the leading candidate for an experiment for this IR. The detector includes precision vertex detectors (microstrips or smart pixels) which must be placed very close to the beam line. This implies a minimal beam pipe, so the question of minimum "stay-clear" distance in this IR must also be addressed. Although this matter has also been discussed elsewhere [3], we summarize the results here as well.

2. Essentials

The motion of a particle as it travels around the machine is usually described by the betatron amplitude functions $\beta_x(s)$ and $\beta_y(s)$, where s is distance around an equilibrium orbit. They have units of length, taken as meters for the present discussion. The envelope of transverse oscillations at a given point is proportional

to $\sqrt{\beta}$; more specifically,

$$\sigma^2 = \beta\epsilon_N/\gamma \ , \tag{1}$$

where ϵ_N is the "normalized emittance" (nominally 10^{-6} m-rad at the SSC), and γ is the usual Lorentz factor (2.13×10^4 for 20 TeV protons). β reaches a minimum value $\beta^\star$ at the interaction point, and grows quadratically with distance ℓ in the drift space from the IP to the entrance of the first element of the triplet:

$$\beta \approx \beta^\star + \ell^2/\beta^\star \tag{2}$$

These may be combined to obtain

$$\sigma^2 = \sigma^{\star 2}\left(1 + (\ell/\beta^\star)^2\right) \ , \tag{3}$$

where β and σ without subscripts refer to either the x or y directions. Inside the triplet the behavior of β is determined by the quadrupole field gradients, and it reaches a maximum value $\hat{\beta}$.

If the beams collide head-on, the luminosity is given by

$$\begin{aligned} \mathcal{L}_0 &= \frac{N_B^2 c}{4\pi\sigma^{\star 2} S_B} \\ &\propto \frac{1}{\beta^\star} \ . \end{aligned} \tag{4}$$

The luminosity is somewhat decreased if there is a finite crossing angle α; this case is discussed below.

The standard SSC lattice is now the 90° lattice described in Ref. 4 rather than that described in the CDR. We use values for the new lattice for purposes of this report.

3. Maximum luminosity

The two sets of quadrupoles on each side of an interaction region function just as a zoom lens does in an optical system, with the effective focal length being long during injection and minimal during collision. The final triplet does little more than focus a parallel beam to a point at the IP, and it is the other triplet which mostly determines the effective focal length and hence how small the spot is—how small $\beta^\star$ is. Rays converge more rapidly in the small-$\beta^\star$ case, and since the distance is fixed must have a bigger excursion ($\hat{\beta}$) in the final triplet. If the effective focal length of this triplet is f, then

$$\beta^\star\hat{\beta} = 1/f^2 \ .$$

In the thin-lens approximation, we would expect the distance $L^\star$ from the IP to the triplet entrance to be f minus half the physical length of the triplet, which

can be easily calculated given the particle momentum and the maximum available gradient.

For example, $\beta^\star\hat{\beta} = (63\ \mathrm{m})^2$ for the high-luminosity IR described in the CDR. The physical length of the triplet is almost 53 m, so we should expect $L^\star = 36.5$ m. In practice, it is 20 m. The difference comes about because the thin-lens approximation is so bad in this case; it becomes better as f increases. In practice, the best way to proceed is via a numerical calculation.

Johnson explored the small-$\beta^\star$ case at Snowmass in 1986 [5]. His motive was to find if better quadrupole placement could result in an even smaller $\beta^\star$ in a high-luminosity IR. Calculations were made for a series of configurations, ranging from $L^\star = 12.5$ m to $L^\star = 75.5$ m. He found that $\beta^\star$ went through a minimum at $L^\star = 20$ m. (We do not regard this as too surprising, because the insertion optics had been carefully optimized for minimum $\beta^\star$ at this $L^\star$.) He recently added a point at $L^\star = 120$ m. The results are shown in Fig. 1(a), and the luminosity under standard beam conditions is shown in Fig. 1(b).

In all of the calculations $\hat{\beta}$ was constrained to a maximum value of 8 km. There are at least two reasons for doing this: $\hat{\beta}^{1/2}$ is a measure of the beam envelope size in the quadrupole, and as such should be kept small. The contribution of this IR to the machine chromaticity is proportional to the integral of β through the triplet, so this contribution will be smaller if $\hat{\beta}$ is smaller. This in fact is a concern, since the two high-luminosity IRs contribute about half of the machine's total chromaticity, and further contributions are not particularly welcome. It had been hoped that the intermediate-luminosity IRs would not contribute so much, but this will occur if they run at the maximum luminosity attainable for a given $L^\star$.

We are also cautioned that for these calculations parts of the high-luminosity insertion region were simply rearranged, whereas for a real design the insertion region is optimized for each $L^\star$. For a variety of reasons (crossing angle implications for aperture, chromaticity considerations, etc.) the results may be somewhat optimistic. It is fair to conclude that (a) the ($\beta^\star = 0.5$ m, $L^\star = 20$ m) case has been very carefully done, and (b) for $L^\star = 120$ m, the best design probably yields a $\beta^\star$ closer to 5 m than to the 10 m given in the CDR.

4. Crossing angle

For the calculations shown in Fig. 1, a crossing angle $\alpha = 75\ \mu$rad (full angle, not half angle) has been assumed. A variety of constraints on this angle have been discussed elsewhere, and are shown in Fig. 2 [6].

Piwinski has pointed out that if the crossing angle is too large, the head-tail interactions of intersecting bunches couple synchrotron and betatron interactions

with undesirable results [7]. The scale factor is proportional to the ratio of horizontal to longitudinal beam size, or

$$\begin{aligned}\alpha_0 &= 2\sigma_0/\sigma_\ell \\ &= 1.96 \text{ mrad} \times \sqrt{\beta^\star/(100 \text{ m})}\,.\end{aligned} \tag{5}$$

The second equation assumes SSC nominal conditions, with $\sigma_\ell \approx 0.07$ m and the other parameters as given in section 2. How rapidly problems appear as the crossing angle increases is unclear, but $\alpha < \alpha_0$ seems to be a reasonable criterion.

The volume of the long, thin bunches actually intersecting also decreases with increasing α, so that the luminosity decreases. Again α_0 is the relevant scale factor, so that if the head-on luminosity is $\mathcal{L}_0$, the actual luminosity is given by

$$\mathcal{L} = \frac{\mathcal{L}_0}{\sqrt{1 + (\alpha/\alpha_0)^2}} \tag{6}$$

Since the beam width $\sigma^\star$ increases with $L^\star$, the correction becomes less important as $L^\star$ increases if the crossing angle is held constant. The actual luminosity $\mathcal{L}$ is plotted in Fig. 1(b). The correction varies from 0.88 at $L^\star = 20$ m to 0.98 at $L^\star = 120$ m.

If bunches substantially interpenetrate at the first encounter after the IP, there is substantial nonlinear disruption and also "satellite luminosity" sources. The CDR uses $> 7\sigma$ as a criterion for the first problem, and with this separation there is negligible satellite luminosity. This *lower limit* to α is indicated in Fig. 2 by the solid curve with the upward-pointing arrow. Since the required separation scales as σ evaluated at half the bunch spacing, it is proportional to $\sqrt{\beta^\star}$ for small $\beta^\star$ and as $1/\sqrt{\beta^\star}$ for large $\beta^\star$.

The final consideration has to do with tune shifts induced by the long-range interaction of passing bunches. This time the range of summation over encounters depends on $L^\star$, but the dependence on $\beta^\star$ again has the form given by Eq. 2. Curves for two extremes of $L^\star$ are shown in Fig. 2.

The net result is that α should be chose to be less than α_0 but greater than the other two limits. $\alpha = 75$ μrad is barely large enough at $\beta^\star = 0.5$ m, and it is again barely acceptable at $\beta^\star = 5$ m. It cannot be substantially decreased in between, although there is a shallow minimum.

The beam separation increases linearly from the IP to the first quadrupole entrance, reaching a value of 1.5 mm at 20 m and 9 mm at 120 m. This has an impact on the minimum beam pipe size and on the results shown in Fig. 1, since larger-aperture magnets with smaller field gradients may be necessary to accommodate the widely separated beams.

5. Minimal beam pipe size

The minimum allowable size for the beam pipe can be set by a simple criterion: the limiting aperture of the machine should be somewhere else during all phases of the collider operation. It is sufficient to consider the limiting cases of injection and collision. There are three criteria:

1. The distance from the beam centerline to the vacuum pipe wall divided by the beam width as given by Eq. 3 must be less than the minimum value of this quantity elsewhere in the machine. In other words, the wall someplace else must be fewer standard deviations away.
2. During some phases of the operation, the beams have a horizontal separation distance of perhaps 5 mm, so 2.5 mm must be added to horizontal stay-clear distances.
3. The beam centerlines diverge vertically at angle α; appropriate clearance must be included.

The IR beam optics during injection and acceleration are different than during collision, in order to minimize $\hat{\beta}$ until stable conditions are established. As a consequence, $\beta^\star$ and $\sigma^\star$ are much larger during injection than during collision. In addition, the beams are smaller after acceleration because of the change in the Lorentz factor. The optics in the arcs are always the same , with $\beta_{max} = 388$ m, and the beam pipe radius is 1.65 cm.

In the collision configuration $\hat{\beta}$, the maximum amplitude in the triplet, may be as large as 8000 m. A limiting aperture here would be intolerable for background reasons, so scrapers are moved into place elsewhere in the machine. As a result, injection optics still determines the limiting beam pipe dimensions in spite of the larger $\hat{\beta}$ in the collision optics configuration.

The CDR injection energy is 1 TeV, but now that the Illinois site constraint has been removed a 2 TeV high energy booster is being seriously considered. However, criterion 1 above is given in terms of the *ratio* of standard deviations which scale the same way with γ, so the injection energy does not enter this part of the discussion.

Unfortunately, injection optics have not been worked out for any of the $L^\star$'s shown in Fig. 1 except for $L^\star = 20$ m. In this case $\beta^\star_{inj} = 8$ m. For the intermediate $\beta^\star$ described in Ref. 4 (which is similar to that in the CDR), $\beta^\star_{inj} =$ 60 m, or $\sigma^\star = 0.168$ mm at 2 TeV. We conservatively use the latter values for the present purposes.

Our criteria can now be stated more precisely:

1. Let $r_{arc} = 1.65$ cm. From Eq. 1 we find $\sigma_{arc} = 0.426$ mm for the maximum

beam size in the arcs, using $\beta_{max} = 388$ m and γ corresponding to 2 TeV protons. The the limiting $r(\ell)$ is given by

$$r(\ell) = r_{arc}\frac{\sigma(\ell)}{\sigma_{arc}}$$

and may be calculated with the aid of Eq. 3. Any particle outside this radius will have hit the beam pipe in the arcs first! The functions $\sigma(\ell)$ and $r(\ell)$ are given in Table 1.

2. To the limiting beam-wall distance $r(\ell)$ we add 0.25 cm in the horizontal direction (x) to provide for horizontal beam separation. This horizontal centerline-wall distance r_x is also given in the Table.

3. In the vertical direction we add $\alpha\ell/2$ (where $\alpha = 75$ μrad) to allow for the finite crossing angle. This vertical centerline-wall clearance r_y is given in the final column of the Table.

Table 1

Minimum *inside* dimensions of the beam pipe in an intermediate-luminosity interaction region. Alignment errors are assumed to be zero.

Distance from IP	$\sigma(\ell)$	$r(\ell)$	r_x	r_y
0 m	0.168 mm	0.65 cm	0.90 cm	0.65 cm
20 m	0.177 mm	0.68 cm	0.93 cm	0.76 cm
40 m	0.202 mm	0.78 cm	1.03 cm	0.93 cm
60 m	0.237 mm	0.92 cm	1.17 cm	1.15 cm
80 m	0.256 mm	0.99 cm	1.24 cm	1.29 cm
100 m	0.274 mm	1.06 cm	1.31 cm	1.44 cm
120 m	0.291 mm	1.12 cm	1.27 cm	1.57 cm

We also note that the beams are smaller after acceleration by $\sqrt{10}$ because of the change in the Lorentz factor. β reaches a very large maximum (2600 m) in the IR quadrupoles. Since a limiting aperture here would be intolerable for background reasons, scrapers are moved into place elsewhere in the machine. In principle, vertex detectors inside a vacuum pipe could also be moved in during colliding-beam conditions.

Building this rather preposterous beam pipe is another matter. It is out-of-round, typically 2 cm across, and about 150 m long. Moreover, any flanges over most of the length will interfere with the operation of strip or pixel detectors,

the walls must be as thin as is permissible for a vacuum pipe, and it is probably to be made of some esoteric and possibly toxic metal which is nearly impossible to machine or weld.

Acknowledgments

This report would not have been possible without extensive discussions with A. A. Garren and D. E. Johnson. Supplemental calculations were made by D. E. Johnson to extend the results of his original report to $L^\star = 120$ m.

References

1. R. Diebold and D. E. Johnson, "p-p Interaction Regions," *Proc. of the 1984 Summer Study on the Design and Utilization of the Superconducting Super Collider*, ed. by R. Donaldson and J. G. Morfín (Snowmass CO 1984), pp. 399-408.
2. *Conceptual Design of the Superconducting Super Collider*, SSC Central Design Group (J. D. Jackson, ed.), SSC Central Design Group Report SSC-SR-2020 (March 1986).
3. K. J. Foley *et al.*, "Report of the Intermediate $p_\perp$ Detector Group: A Beauty Spectrometer for the SSC," *Proc. of the Workshop on Experiments, Detectors, and Experimental Areas for the Supercollider*, ed. by R. Donaldson and M. G. D. Gilchriese, Berkeley CA July 7-17 (1987), pp. 759-787.
4. A. A. Garren and D. E. Johnson, "The 90° (September 1987) SSC Lattice," SSC Central Design Group Report SSC-146 (1987).
5. D. E. Johnson, "High-Luminosity Insertion Scaling," *Physics of the Superconducting Supercollider*, ed. by R. Donaldson and J. Marx (Snowmass CO 1986), pp 519-520.
6. D. E. Groom, "Long-Range Tune Shifts and Other Matters in High-$\beta^\star$ IRs," SSC Central Design Group Report SSC-88 (1986).
7. A. Piwinski, "Computer Simulation of Satellite Resonances Caused by Beam-Beam Interaction at a Crossing Angle in the SSC," SSC Central Design Group Report No. SSC-57 (1986).

APPENDIX

Qualitative comments about final-focus optics

The main ring of the SSC consists of evenly spaced quadrupoles with alternating gradients. Between them are the dipoles which bend the particles into closed orbits, but these have no major importance in the optics. In the vicinity of each interaction region is an "experimental insertion" which must—

(a) cause the beams to cross at the interaction point (IP);

(b) make β reach a small value $\beta^\star$ at the IP, and permit its value to be tuned for purposes of injection and other beam manipulations;

(c) provide as much free space as possible for experiments (there is a tradeoff between this free space and the minimum value $\beta^\star$ can reach);

(d) and tend to a variety of housekeeping chores such as minimizing dispersion and beam-beam interactions.

An example of such an insertion (for $\beta^\star = 0.5$ m, $L^\star = 20$ m) is shown in Fig. 3. $\beta^\star$ is established by the final-focus triplet (1QD, 2QF [which is split], and 3QD) and a doublet (4QD and an F element which is split into 5QF and 6QF). The other elements have to do with vertical beam bends and dispersion suppression. "F" and "D" mean "focusing" and "defocusing" in the horizontal direction. These functions are reversed in the vertical direction with the same overall result.

Below the figure we show an optical analog for the horizontal direction. The final-focus "lens" is 50 m thick while the distance $L^\star$ from the end to the focal point is only 20 m, so it is hardly a thin lens. However, we treat it as such in the following discussion.

Operation of the triplet during injection (high $\beta^\star$) and collision (low $\beta^\star$) are shown schematically in Fig. 4. Central and limiting rays are indicated by solid lines. The position of an equivalent thin lens and limiting rays through it are shown by dash-dotted lines. In both cases the rays enter or leave the insertion optics on the right in the same way. In both cases the final-focus triplet does little more than focus a parallel beam to a point. In the actual design the current in these elements is changed by only 5% in changing from a high-$\beta^\star$ to a low-$\beta^\star$ configuration at full field.

In the injection and acceleration configuration (high $\beta^\star$), 5QF is fully powered while 6QF is almost off. In the collision configuration (low $\beta^\star$) the situation is reversed. The net effect is that in the high-$\beta^\star$ case the limiting ray has a small excursion in the final-focus triplet (small $\hat{\beta}$) and makes a small angle with the

central ray at the IP; the overall equivalent thin lens has a long focal length and the beam spot size is proportional to this focal length.

The situation is reversed in the low-$\beta^\star$ case, where the current in 5QF is nearly off and that in 6QF is on. The limiting ray leaves 4QD pointed upward, and it makes a very large excursion in the triplet. As a result it crosses the IP at a large angle. The the thin lens equivalent to the system has a short focal length and makes a small beam spot. The size of the envelope in the triplet is proportional to $\hat{\beta}^{1/2}$, and we see that a small $\beta^\star$ of necessity implies a large $\hat{\beta}$.

Finally, what is the role of the quadrupoles between the vertical bend magnets BV1− and BV2+? Consider a ray which leaves the IP on axis but with slightly less than the nominal momentum. It is bent upward a little too far by BV1+, and is bent back to horizontal above the closed orbit by BV1−. If the vertical bend were done in one step it would enter the machine lattice with this displacement, translating dispersion into the excitation of betatron oscillations. However, the string of quadrupoles is designed to reverse the situation: If the particle enters the quadrupoles above the equilibrium orbit, it leaves the string below the equilibrium orbit by the same amount. The second set of vertical bends (BV2) does the same thing as the first, but this time brings the off-momentum particle into the machine lattice without displacement.

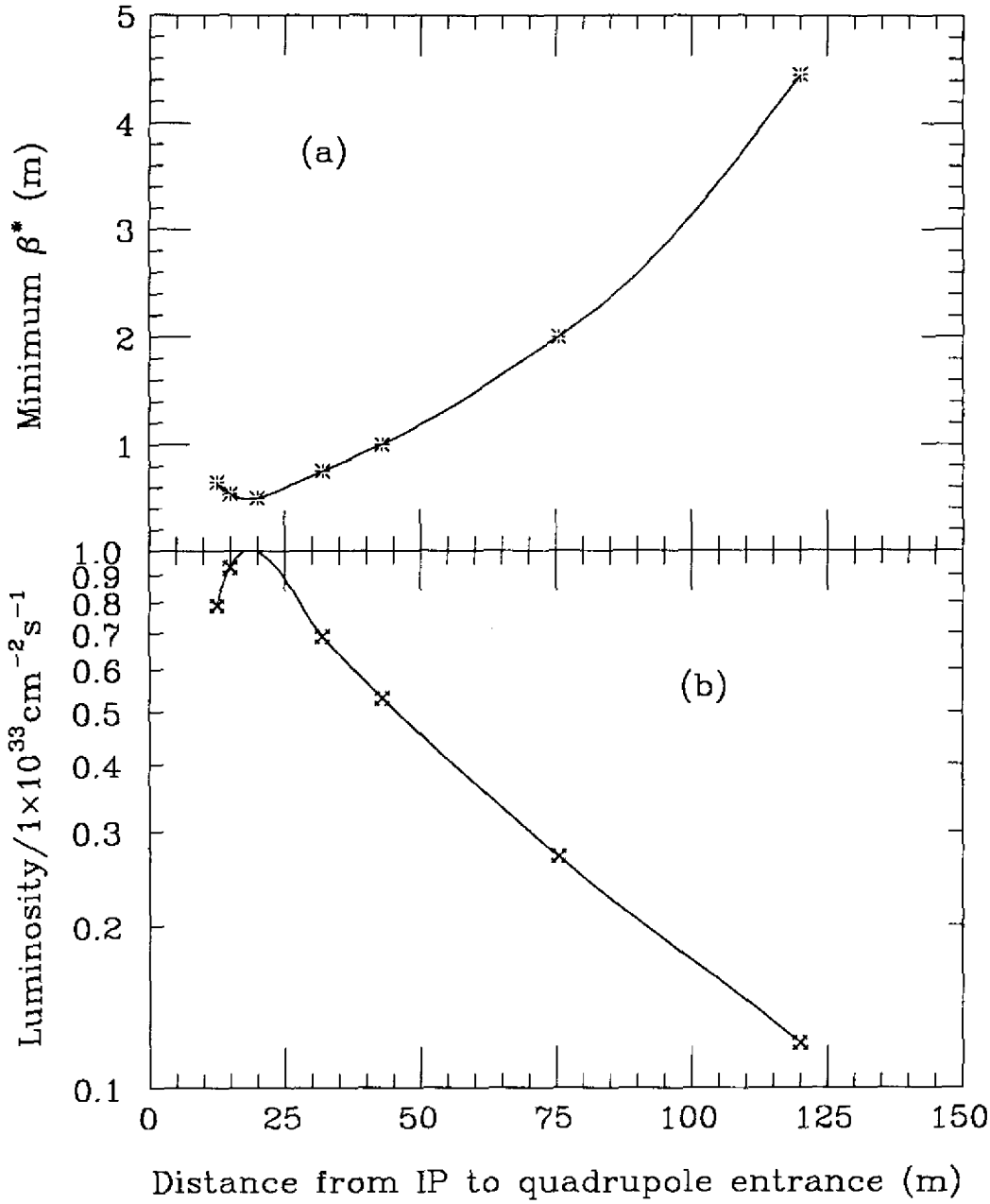

FIG. 1. $\beta^\star$ (a) and luminosity (b) as a function of $L^\star$ as given in Ref. 1 and by more recent calculations. The model is somewhat artificial, and may be optimistic for $L^\star > 20$ m.

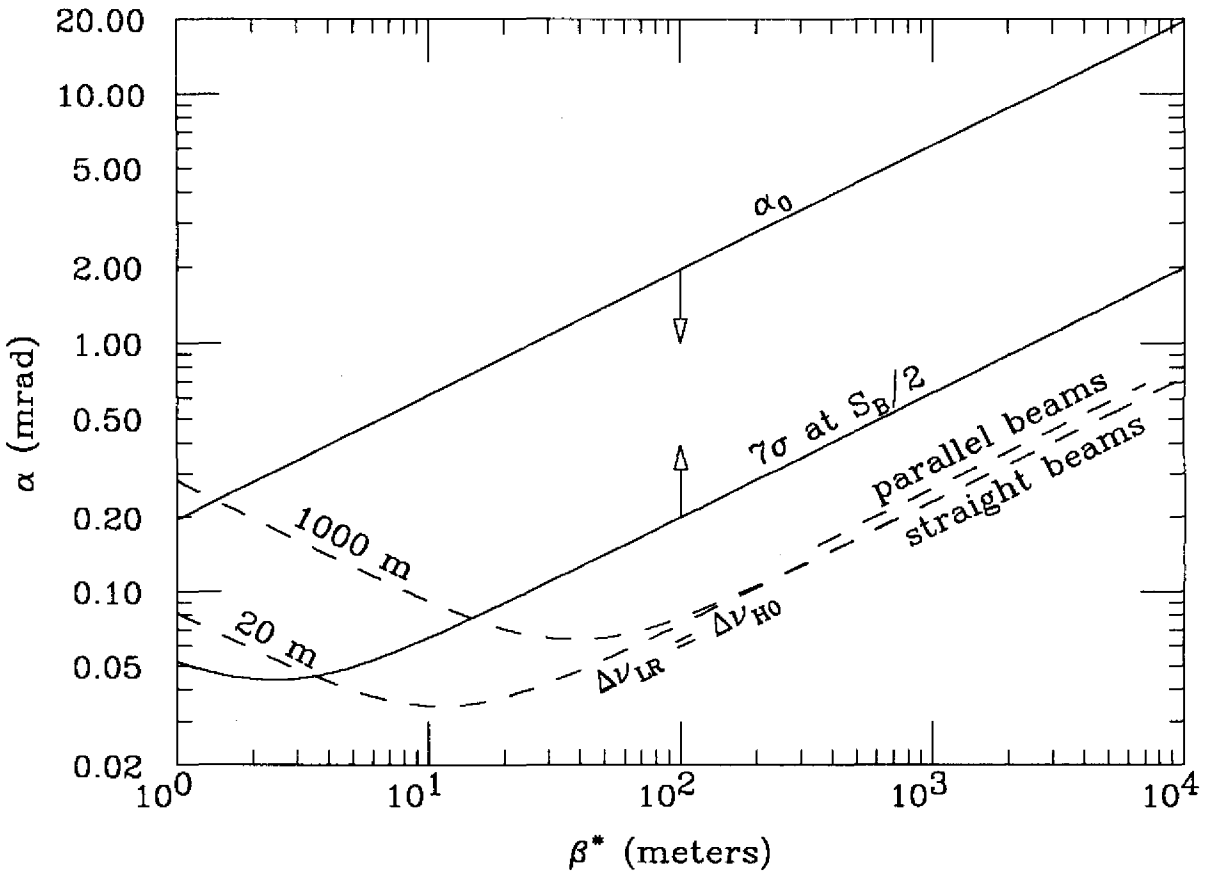

FIG. 2. Various limits on the crossing angle α as a function of $\beta^\star$. Lower limits are marked by upward arrows; the upper limit is indicated by a downward arrow. The distances on the dotted lines refer to free space between the IP and triplet entrance ($L^\star$).

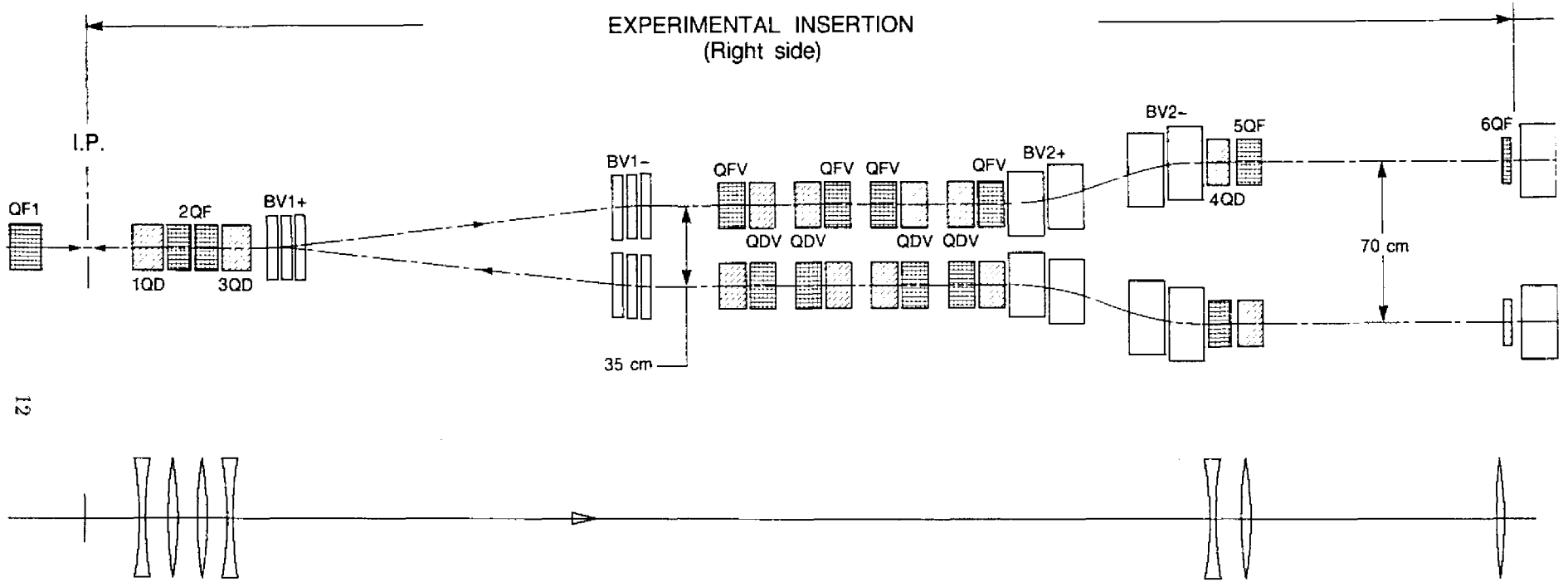

FIG. 3. The low-β^* experimental insertion for the SSC. An optical analog for the relevant optics is shown below for the horizontal direction for a beam traveling from left to right. Focusing and defocusing elements are interchanged for the vertical direction or for beams traveling from right to left, but the overall function of the triplets and doublets is unchanged.

(a) High-$\beta^\star$ injection optics

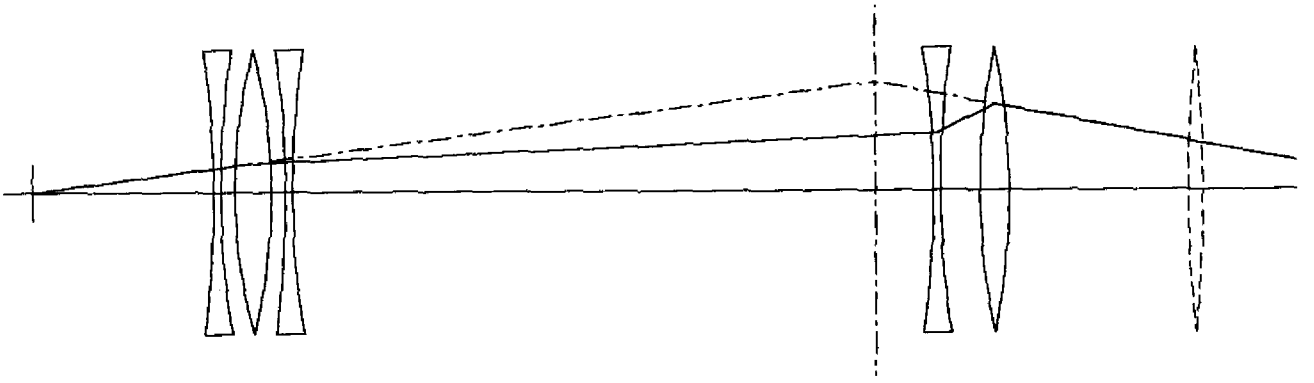

(b) Low-$\beta^\star$ collision optics

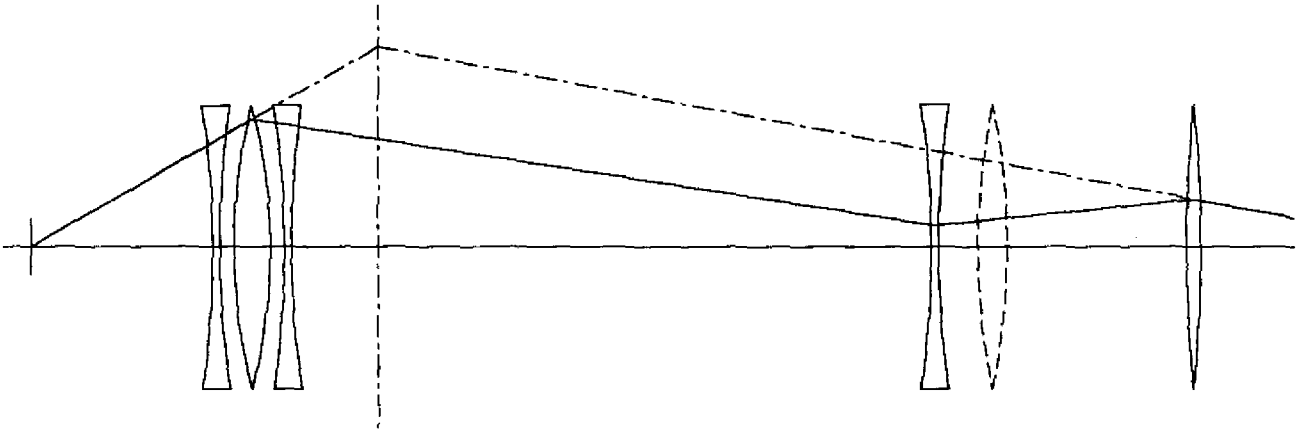

FIG. 4. Qualitative optical analog for the operation of experimental insertion optics for (a) injection and acceleration, and (b) collision. The position of an equivalent thin lens may be found by extrapolating entering and exiting rays, and is shown in each case by the vertical dash-dotted line.